Analytica Chimica Acta 686 (2011) 126–132

Contents lists available at ScienceDirect

Analytica Chimica Acta

journal homepage: www.elsevier.com/locate/aca

# Use of microperoxidase-11 to functionalize tin dioxide electrodes for the optical and electrochemical sensing of hydrogen peroxide

Yeni Astuti[a], Emmanuel Topoglidis[b,*], James R. Durrant[a]

[a] Department of Chemistry, Imperial College, Exhibition Road, London SW7 2AY, United Kingdom
[b] Department of Materials Science, University of Patras, Patras 26504, Greece

ARTICLE INFO

*Article history:*
Received 2 September 2010
Received in revised form
17 November 2010
Accepted 22 November 2010
Available online 30 November 2010

*Keywords:*
Microperoxidase-11
Hydrogen peroxide
Biosensor
$SnO_2$ electrodes

ABSTRACT

In this paper, we employ microperoxidase MP-11 immobilized on mesoporous $SnO_2$ electrodes in order to study its peroxidase activity and reaction mechanism. We demonstrate the catalytic redox chemistry of the immobilized MP-11 via direct interfacial electron transfer without the use of electron mediators. By taking advantage from the optical transparency of the $SnO_2$ electrodes, optical absorbance spectroscopy is used in order to compliment the data information obtained from electrochemical techniques. The catalytic activity of the immobilized MP-11 is found to proceed via the Fenton reaction, yielding OH radical intermediates. We also demonstrate the viability of using this electrode system as a potential $H_2O_2$ biosensor with a sensitivity range of 0.05–30 μM.



## 1. Introduction

Heme-containing proteins such as peroxidases and cytochromes have many potential uses and applications in the fields of biosensors and biocatalysis [1,2]. In the last 20 years, there has been considerable interest in the direct electron transfer between redox proteins and electrode surfaces [3]. Many immobilization methods were developed to fabricate protein electrodes, such as sol–gel [4–6] and self-assembled techniques [7,8]. By studying proteins immobilized on surfaces, one can obtain valuable information on the mechanisms of biological electron transfer. For example, the electrochemistry of microperoxidase 11 (MP-11) has been well studied. MP-11 is proposed as a potential candidate to replace horseradish peroxidase (HRP) in its major applications. This hemepeptide offers some advantages such as simpler design, smaller size and commercial availability.

MP-11 is a small size redox enzyme obtained by proteolytic digestion of cytochrome-*c* (Cyt-*c*) [9]. It is an oligopeptide consisting of eleven amino acids and a covalently linked FeIII – protoporphyrin IX heme. The hemepeptide is soluble in water with IEP of 4.7 [10,11]. Even though the peroxidase activity of MP-11 has been reported more than 60 years ago [12], its mechanism has yet to be fully understood. It has been promoted to replace Horseradish peroxidase (HRP) as it has been found to have a peroxidase activity, as it can catalytically reduce $H_2O_2$ to $H_2O$ [13]. However, little has been known about the MP-11 reaction mechanism. Some reports showed that this minienzyme undergoes the classic peroxidase cycle [14], while others show data indicative of a different mechanism [15], most probably Fenton chemistry.

The electrochemical and electrocatalytic properties of MP-11 have been studied using different electrodes. Several reports showed that MP-11 maintained its peroxide sensitivity upon immobilization on a number of electrode materials such as ITO conducting glass [16], silver [17], gold [14,18–20], graphite [21], carbon paste [21], glassy carbon [22,23], single walled carbon nanotubes [24,25] and multi-walled carbon nanotubes [26]. The immobilization strategy includes the physical adsorption on electrodes modified with either DDAB [15], nano-zinc oxide [27] or chitosan [22] and polyion complex membranes consisting of poly-L-lysine (PLL) and poly(4-styrene sulfonate) [28]. Covalent attachment of MP-11 using cystamine [14] and glutaraldehyde [29] has also been reported.

Wiring of redox enzymes on electrode surfaces by different immobilization techniques is of great interest, as fast electron transfer between the electrode surface and the redox centre of the protein can be achieved [30]. By using MP-11 in particular, the denaturing adsorptions of the proteins are limited, a better understanding of the redox properties of the enzyme can be achieved and enzyme biosensors can be developed. A lower detection limit for hydrogen peroxide as small as 0.5 μM has been reported for immobilized MP-11 [16,28]. However this figure has not yet reached that of nanomolar range achieved with HRP and cytochrome *c*

* Corresponding author. Tel.: +30 2610 969924; fax: +30 2610 969368.
*E-mail address:* etop@upatras.gr (E. Topoglidis).

0003-2670/$ – see front matter © 2010 Elsevier B.V. All rights reserved.
doi:10.1016/j.aca.2010.11.045

peroxidase (CcP) [31,32], indicating that more effort must be done to improve MP-11 performance for it to be useful in electroanalytical applications.

Herein we describe the electrochemistry of MP-11 immobilized on mesoporous $SnO_2$ electrodes. In the past we managed to immobilize Cyt-*c*, Hemoglobin and HRP successfully on these electrodes and developed optical and electrochemical biosensors [33,34]. Nanocrystalline $SnO_2$ films are more conducting than either ZnO or $TiO_2$ films. This metal oxide exhibits a band gap (330 nm) and an isoelectric point of IEP∼5 similar to those of $TiO_2$ [34]. We immobilized MP-11 on these electrodes in order to determine the mechanism of the peroxidase activity of MP-11 in our experimental system and to demonstrate the viability of using this electrode system as a potential electrochemical biosensor.

## 2. Experimental

### 2.1. Chemicals

MP-11 from horse heart Cyt-*c*, poly-L-Lysine (PLL) (MW: 500-2000), poly(ethyleneimine) (PEI) (average $M_n$: 1200), didecyldimethylammonium bromide (DDAB) (MW: 406,53) and coumarin were purchased from Sigma–Aldrich. $H_2O_2$ stock solution (10 mM or 100 μM) was prepared by diluting $H_2O_2$ (30%, BDH Aristar) in deionised water. The concentration of $H_2O_2$ was verified by optical measurements at 240 nm ($\varepsilon_{240} = 40\ M^{-1}\ cm^{-1}$) [35–37]. All aqueous solutions were prepared in distilled, deionised water of resistance $R = 15\ \Omega$ cm.

### 2.2. Instrumentation

Electrochemical and spectroelectrochemical experiments were performed using an Autolab PGStat 12 potentiostat and a Shimadzu UV-1601 spectrophotometer. The spectroelectrochemical cell was a 4 mL, three-electrode cell with quartz windows, employing a platinum mesh flag as the counter electrode, a Ag/AgCl, KCl [3.5 M] reference electrode and the $SnO_2$ electrode as the working electrode. All potentials are reported against Ag/AgCl. The electrolyte solutions used were 3 mL of 10 mM PBS of pH 8, which was deoxygenated with Argon prior any optical/electrochemical measurements. For spectroelectrochemistry, the above cell was incorporated in the sample compartment of the spectrophotometer and the absorption changes monitored as a function of step or sweep potential. Then, the absorbance at any wavelength indicating electron transfer were differentiated with respect to the potential, followed by smoothing with a fast Fourier transform smoothing algorithm. All experiments were carried out at room temperature.

### 2.3. Procedures

#### 2.3.1. Preparation of $SnO_2$ electrodes

The $SnO_2$ paste, consisting of 15-nm-sized particles, was prepared following a sol–gel procedure: 345 mL of distilled water was used in a 500-mL glass beaker in a cooling bath (∼−5 °C). A total of 10.8 mL (equivalent to 24 g) of $SnCl_4$ was then slowly added and left stirring until the solution became clear and the amount of $SnO_2$ in the solution was ∼4%. A dialysis membrane (Membra-Cel TM MD34-14.100 Clear) was used to separate the colloids. The sol–gel was then acidified to pH 1 with $HNO_3$ prior to autoclaving at 230 °C for 12 h. The solution was then concentrated to 12% before precipitating the $SnO_2$ with ethanol. After this, the colloidal solution was prepared for spreading on conducting glass slides. We used a 20% $SnO_2$ paste mixed with 7.3% ethylcellulose 7 mPa, 2.7% ethylcellulose 45 mPa, and 70% terpineol and ethanol as the solvent. The solution was stirred and sonicated until it became homogeneous. The ethanol was removed by the use of a rotor evaporator using a vacuum pump at 40 °C. The $SnO_2$ suspension was then applied to the surface of a conducting glass using the "doctor blade" technique. Masking the glass slide with Scotch tape controlled the thickness and the width of the area spread, with one layer of tape being employed to yield a final film thickness of 4 μm. The spread suspension was then allowed to dry before being sintered for 20 min at 450 °C. The thickness of the mesoporous $SnO_2$ films was measured with a DEKTAK profilometer. The $SnO_2$ films were cut in 1 $cm^2$ pieces. Immediately prior to enzyme immobilization, the films were heated to 450 °C for 15 min and then allowed to cool down to room temperature before being immersed in the protein solution. Modification of $SnO_2$ electrodes was achieved by immersing them overnight in 20 μM poly-L-lysine (PLL), a polycationic binding promoter solution.

#### 2.3.2. MP-11 immobilization

Aqueous solutions of MP-11 were prepared in 10 mM sodium phosphate (PBS) buffer of pH 6, 6.5, and 7, respectively. Prior to immobilization, a piece of $SnO_2$ electrode was heated at 450 °C for 20 min to remove all the dirt and any adsorbed water. After cooling, the electrode was immersed in MP-11 solution and the protein adsorption was followed by monitoring the optical absorbance change over one week. Strong absorption was only observed following modification of $SnO_2$ electrodes by immersing them in polycationic binding promoter solutions overnight, either 20 μM poly-L-lysine (PLL), 15 μM poly(ethyleneimine) (PEI) or 20 μM didecyldimethylammonium bromide (DDAB).

The modified $SnO_2$ electrodes were then rinsed with PBS buffer and immersed in MP-11 solution at 4 °C for the required length of time. Contributions to the spectra from the scatter and absorption by the $SnO_2$ electrode alone were subtracted by the use of protein free reference electrodes. Prior to all spectroscopic measurements, electrodes were removed from the immobilization solution and rinsed in buffer solution to remove non-immobilized protein.

#### 2.3.3. Electrochemical sensing

The $H_2O_2$ solution was titrated into the electrochemical cell using a GSE microsyringe. Electrochemical biosensing was performed by the chronoamperometric technique, monitoring the increase in catalytic current after titration into the cell of hydrogen peroxide. All experiments were carried out at room temperature.

#### 2.3.4. Hydroxyl radical assay with coumarin

The presence of hydroxyl radicals was assayed by the formation of a highly fluorescent product upon its reaction with coumarin [38–42]. A stock solution of 10 mM coumarin was prepared by adding coumarin to 1 mM $H_2SO_4$ and left stirring overnight. A typical assay employed 40 μM coumarin, 100 μM $H_2O_2$, in 10 mM PBS pH 6 as electrolyte in the electrocatalytic system. A potential of −400 mV was applied to the MP-11/$SnO_2$-PLL electrodes for 30–100 min in the presence of this electrolyte. The fluorescene spectra were measured using a PerkinElmer LS-50 spectrofluorimeter with an excitation wavelength of 332 nm.

## 3. Results

### 3.1. MP-11 immobilization

Immobilization of MP-11 results in orange-brown coloration of $SnO_2$ electrodes. PLL pre-modification was found to be necessary to promote MP-11 immobilization since in the absence of this promoter, no significant MP-11 was observed on the electrode surface. Typical UV visible absorption spectra are shown in Fig. 1 in comparison with the respective spectra of MP-11 in the solution.

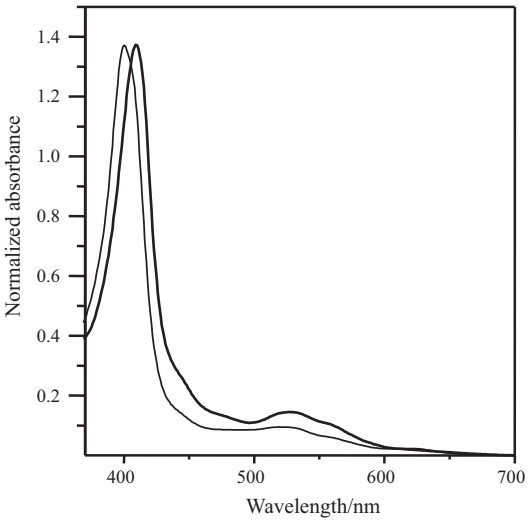


**Fig. 1.** UV–vis absorption spectra of MP-11 in solution (—) and immobilized on metal oxide electrodes (—). PLL is employed in MP-11 immobilization.

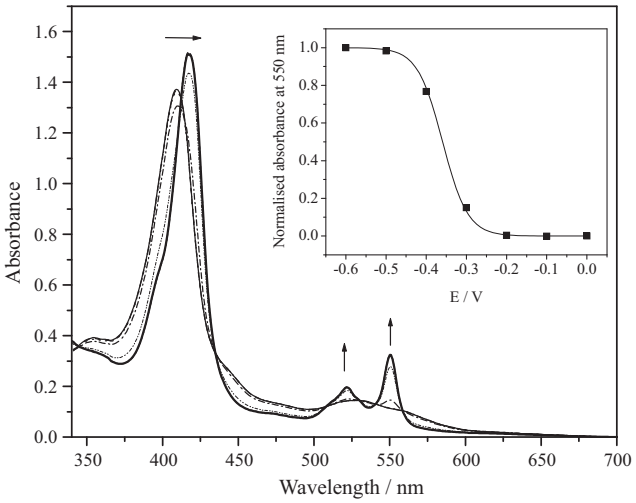


**Fig. 3.** UV–vis spectral changes for the formation of ferrous MP-11 (—) on $SnO_2$-PLL after applying step potentials of −0.1 V every 2 min. The inset shows the clean fitting of data to the one electron Nernst equation.

The characteristic 400 nm band observed for MP-11 in solution is red shifted to 409 nm upon immobilization on a PLL modified mesoporous $SnO_2$ electrode. Interestingly, a similar observation was also reported by [15] following the binding of MP-11 to DDAB, a cationic lipid vesicle. This shift indicates that the heme microenvironment in immobilized MP-11 is distinctly different from that in the solution, indicative of low spin iron centre. The results of [43] showed that covalent binding of MP-11 to silica support results in monomer MP-11, which retains the high spin iron centre properties. Moreover, Goldston showed that imidazole can bind to the accessible vacant ligand site on the covalently immobilized MP-11, which was marked by a red shift of the Soret band to 406 nm [44]. We furthermore investigated the effect of PLL on this red shifted behaviour by titrating the MP-11 solution with PLL solution. As can be seen from Fig. 2, the Soret band of MP-11 is red shifted as far as 8 nm in the presence of PLL. Similar red shifted spectra were reproduced upon titration of MP-11 with other polycations, i.e. PEI and DDAB. We therefore attribute the red shift observed for immobilized MP-11 to the formation of low spin heme iron centre in the presence of these polycations. Assuming that the absorption strength of MP-11 is similar both in the immobilized and dissolved state, an extinction coefficient of 176,000 $M^{-1}$ $cm^{-1}$ [16] was employed to estimate the amount of protein adsorbed on the surface. This resulted in an approximate MP-11 loading of 9 nmol $cm^{-2}$ on a 4 μm thick $SnO_2$-PLL electrode.

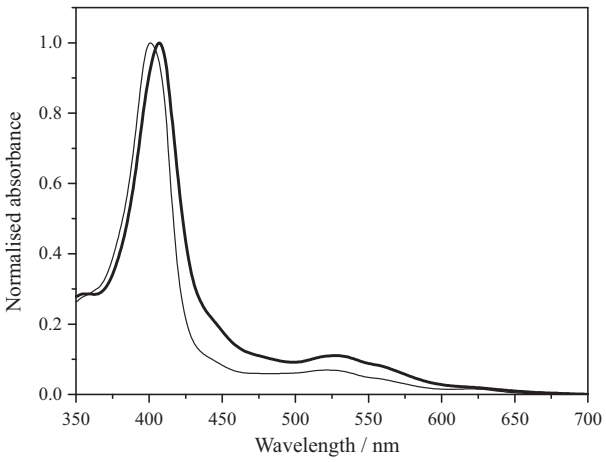


**Fig. 2.** Change in the absorption of MP-11 in 10 mM PBS buffer solution pH 7 (—) upon addition of PLL (—).

### 3.2. Redox function

Having immobilized the MP-11 on the mesoporous $SnO_2$ electrodes successfully, the ability of the enzyme to retain its redox function after immobilization was examined. This was initially done by spectroeletrochemistry experiments and subsequently by cyclic voltammetry experiments.

Typical spectroelectrochemical spectra are shown in Fig. 3. Under application of step potentials, the ferric MP-11 undergoes a progressive one electron reduction forming ferrous MP-11, as marked by clear isosbestic points, a shift in Soret band to 417 nm and the appearance of new bands at 522 nm and 550 nm. These features are characteristic of low spin ferrous hemeproteins as normally observed in Cyt-*c*, in contrast to the expected high spin one for five coordinated ferrous hemeprotoporhyrins as observed on monomeric microperoxidase 8 (MP-8) [45] or native peroxidases. This observation however corroborates the low spin six coordination heme status suggested by the spectrum of its ferric states.

Each spectrum was taken 2 min after applying a step potential to ensure that the redox couple reaches equilibrium. From the fitting of the data to the one electron transfer Nernst equation, the midpoint potential for MP-11 Fe(III)/Fe(II) redox transition was determined to be $-0.350 \pm 0.005$ V. This value is closer to the electrochemistry of hemin of −0.342 V [46] than that of −0.377 V reported previously in solution studies [13] and on gold electrodes [44].

Cyclic voltammetry and cyclic voltasorbtometry are furthermore employed to study the kinetics of electron transfer. CVs of MP-11 immobilized on $SnO_2$-PLL electrode show nearly reversible, well defined cathodic and anodic peaks, attributed to heme reduction and oxidation (Fig. 4). This was verified spectroscopically by measuring the absorbance at 550 nm, characteristic wavelength for the reduced MP-11 [45]. Differentiation of the absorbance signal (DCVA) results in a response that has the same morphology as the CV data, as previously discussed for DCVA's of Cyt-*c* and Fld [47]. The midpoint redox potential of immobilized MP-11 was determined from these data to be −0.357 V, the same within error as the potentiometric spectroelectrochemical data.

The peak current area measured in the CV corresponds to the amount of charge transferred to the electrode and therefore the

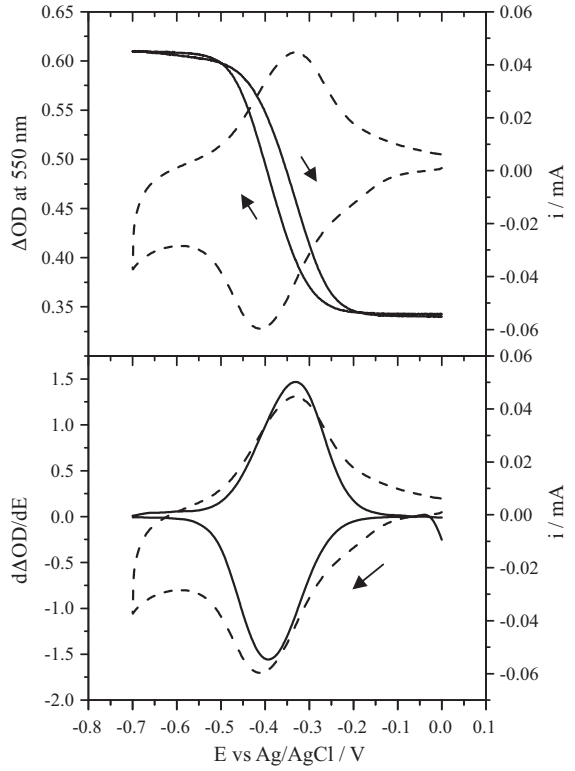


**Fig. 4.** CVs (- - -) of MP-11/$SnO_2$-PLL in comparison with CVA (—, top) and DCVA (—, bottom). Arrows show the scan directions. All experiment was measured at 10 mV $s^{-1}$ in a MP-11 free 10 mM PBS buffer solution of pH 8.

amount of adsorbed protein that participates in the interfacial electron transfer. Comparison of this data with the spectroscopy data of immobilized protein gives estimation that more than 90% (8.3 nmol) of the immobilized MP-11 is electroactive.

The plot of current vs scan rate, inset of Fig. 5, shows a linear correlation for scan rates up to 1 V $s^{-1}$. This indicates the involvement of a surface confined electroactive species, which in turn allows the use of Laviron model to analyse the kinetics of heterogeneous electron transfer [48]. A plot of peak separations vs scan rates is shown in Fig. 5. A linear regression analysis was performed in the data where peak separations are more than 100 mV. Charge transfer

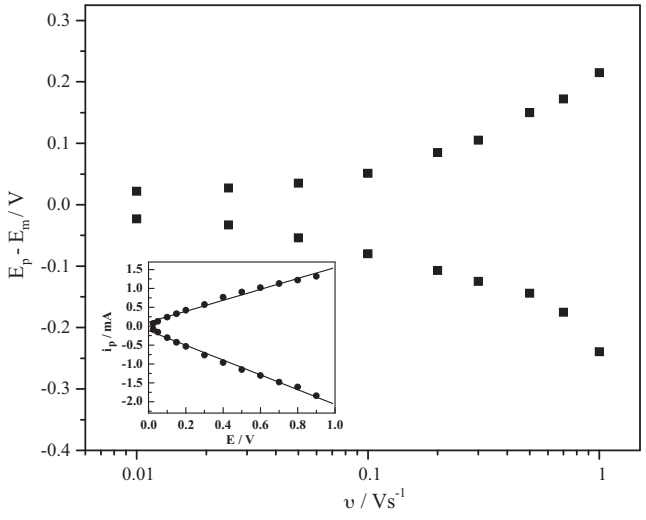


**Fig. 5.** Plots of anodic and ctahodic peak separations against the logarithm of the scan rate for MP-11 (■). The inset show plots of the cathodic and anodic peak currents vs scan rate for MP-11.

**Table 1**
Midpoint potentials of MP-11 upon immobilization.

| Binding promotors | $E_m$ (V) |
|---|---|
| PLL | −0.357 |
| PEI | −0.362 |
| DDAB | −0.230 |
| Solution | ~(-)0.377 [2] |

coefficient, $\alpha$, of 0.50 ± 0.05 is employed and a value of 2.2 ± 0.2 $s^{-1}$ is obtained for interfacial electron transfer rate constant of MP-11 on $SnO_2$-PLL, less than that of 10 $s^{-1}$ for MP-11 covalently attached to gold electrodes [49].

Furthermore, the effect of the binding promoters on the mid point potential was studied, as these are expected to influence the immediate microenvironment of the immobilized MP-11. The $SnO_2$ electrodes were treated with PEI and DDAB before MP-11 immobilization, and the resulting electrodes were then subject to CV measurements.

The midpoint potentials obtained are tabulated in Table 1. As can be seen, the midpoint potential of MP-11 shifted to a more positive value upon binding on DDAB modified $SnO_2$ electrodes. A similar trend was also reported by Huang when studying MP-11 immobilized on DDAB modified PEG electrodes [15]. Moreover, Rusling also reported a positive shift of $E_m$ of several proteins immobilized on electrodes modified with this cationic lipid film [50,51].

### 3.3. Catalytic activity

In contrast to our recent studies on cytochrome *c* peroxidase (CcP) and horseradish peroxidase (HRP) [34], with MP-11 we cannot identify the species involved in the classic peroxidase cycle upon reacting either immobilized or aqueous solution of MP-11 with $H_2O_2$ (Fig. 6). The α and β bands characteristic of oxyferryl species that were observed for CcP and HRP [34] do not appear. Instead, the Soret band continues to bleach with increasing addition of $H_2O_2$ and this bleaching is not reversible.

Electrochemical experiments were furthermore conducted to obtain more information on the catalytic activity of the immobilized MP-11. Considering the peroxidase/electrode systems as an electrochemical analogue of the native peroxidase cycle, catalytic currents are expected to be registered around the formal potential of Compound I/II and compound II/HRP($Fe^{3+}$), which were determined to be in the range of 0.7–0.73 V [53]. However, in our electrode system, the working potential window of the $SnO_2$ electrode that we used herein start from around 0.3 V, limiting the observation of the expected electrocatalytic currents. Cyclic

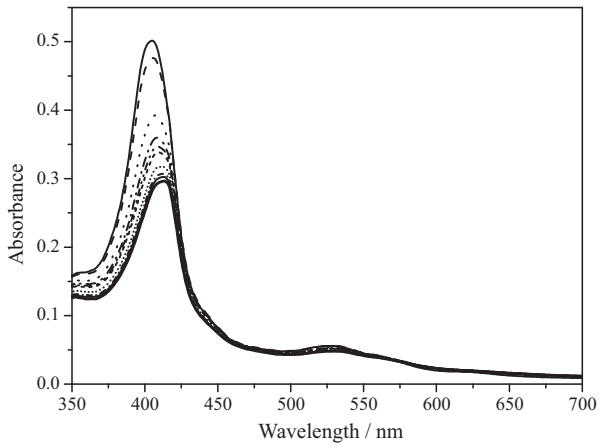


**Fig. 6.** Changing of solution spectrum of 5 μM MP-11 solution upon addition of $H_2O_2$.

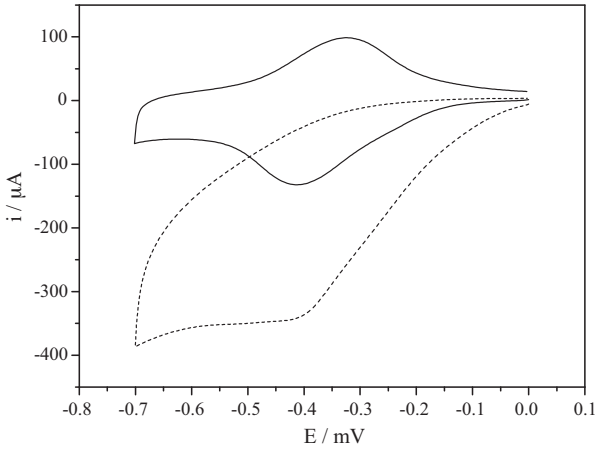


**Fig. 7.** (a) Cyclic voltammograms of MP-11/$SnO_2$-PLL electrodes in 0.01 M phosphate buffer, pH 8.0, scan rate 25 mV $s^{-1}$, (—) without $H_2O_2$, (- - -) in the presence of 40 μM $H_2O_2$.

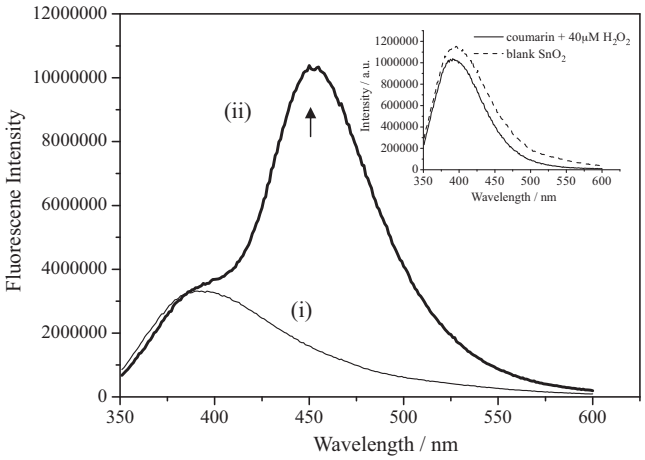


**Fig. 8.** The fluorescence spectra of coumarin in the presence of 40 μM $H_2O_2$ and MP-11/$SnO_2$-PLL electrodes before (i) and after (ii) the application of −0.4 V potential. Excitation wavelength: 332 nm, slit 5. Application of potential at −0.3 V for 100 min to the $SnO_2$-PLL alone does not induce the change in coumarin fluorescence spectrum as shown in inset.

voltammogram obtained using MP-11/$SnO_2$-PLL electrodes in the presence of $H_2O_2$ is shown in Fig. 7. An electrocatalytic current is observed in the presence of $H_2O_2$. No electrocatalytic current is registered at 0 V using MP-11/$SnO_2$-PLL in the presence of $H_2O_2$. Instead, a strong electrocatalytic current is only observed as the applied potential approaches that of MP-11 Fe(III)/Fe(II) redox transition. This behaviour was also observed upon employing DDAB and PEI as binding promoters (data not shown). Moreover, a similar observation was also reported by [15] employing MP-11 immobilized on DDAB modified carbon electrodes. These data, however, are in contradiction with those reported for MP-11 covalently attached to gold electrodes [49] in which the catalytic current was observed at potentials more positive than the midpotential of ferri/ferrous redox couple (+0.2 to 0.3 V), indicating the involvement of iron oxo species in the MP-11 peroxidatic catalytic activity.

In this paper for the MP-11 modified electrode, the Fe(II)/Fe(III) redox transition seemingly plays a direct role in catalytic activity, indicating classical Fenton type reactivity, whereas in HRP and CcP modified electrodes, the classic peroxidase enzymatic activity may be applied as we showed previously [34].

The direct involvement of the Fe(II)/Fe(III) redox transition of MP-11 iron centre in $H_2O_2$ catalysis could involve the formation of hydroxyl radical as indicated in Fenton reaction. Further experiments were therefore undertaken to assay the presence of hydroxyl radicals that may have been formed in MP-11/$SnO_2$-PLL electrocatalytic system. Coumarin was added as a hydroxyl radical scavenger following a method that is widely used in radiation chemistry [39], sonochemistry [40], electrochemistry [42] and photocatalysis [52]. Coumarin solution alone gives a fluorescene at 380 nm however the specific reaction of Coumarin with hydroxyl radicals yields a hydroxylated product, 7-hydroxycoumarin which exhibits a strong emission maximum at 453 nm [39,42].

Fig. 8 indeed shows the appearance of a 453 nm emission band following incubation of coumarin in a solution including $H_2O_2$ and contacted to the MP-11/$SnO_2$-PLL electrode poised at −0.4 V vs Ag/AgCl, confirming the generation of hydroxyl radicals. The possibility of direct oxidation of coumarin was ruled out as no oxidation response of coumarin in electrolyte solution using bare $SnO_2$-PLL electrode was observed at this potential. Similarly, the possibility of oxidation by iron oxo species was ruled out by the fact that no hydroxylated coumarin was formed by incubating the coumarin with MP-11/$SnO_2$-PLL electrode over night in the presence of $H_2O_2$. This hydroxyl radical assay therefore confirms that the MP-11/$SnO_2$-PLL electrocatalytic system proceeds through the Fenton reaction.

### 3.4. Electrochemical biosensor

For the development of electrochemical biosensors, the electrocatalytic current response can be titrated against successive additions of $H_2O_2$. The working electrode of MP-11 modified $SnO_2$-PLL electrodes was held at −0.2 V vs Ag/AgCl in a stirred cell containing 3 mL 0.01 M PBS buffer pH 8. To this cell, aliquots of a 100 μM or 10 mM $H_2O_2$ stock solution were added in order to make it up to a given concentration. Typical chronoamperometric responses are shown in Fig. 9(a). The current became increasingly negative as larger aliquots of $H_2O_2$ were added to the stirred cell, the response time is below 30 s. In order to obtain a calibration curve as shown in Fig. 9(b), the current responses were inverted to a positive value and then plotted as a function of $H_2O_2$ concentration. This figure clearly shows that the MP-11 modified $SnO_2$-PLL electrode is more sensitive than that of HRP reported previously (data also shown in Fig. 9(b)) [34]. The sensitivity of the former was found to be 4.3 A $M^{-1}$ $cm^{-2}$, four times higher than the latter. Moreover, the $SnO_2$-PLL blank electrode shows insignificant response to $H_2O_2$ additions. A linear relationship was obtained in the calibration curve, in a range of 0.05–30 μM and 1–20 μM $H_2O_2$ for MP-11 and HRP modified $SnO_2$-PLL electrode respectively. The lower detection limit is 50 nM, 20-fold lower than the value reported by Tatsuma and Watanabe [16] employing MP-11 immobilized at a flat $SnO_2$ surface. The superior activity of MP-11 on our electrode is most probably due to the higher protein loading evident in our mesoporous electrode. The overall activity of our electrode is also comparable to the best HRP modified electrode, employing Histidine tagged recombinant HRP [54].

## 4. Discussion

The above data have demonstrated our ability to address the catalytic redox chemistry of MP-11 immobilized on mesoporous $SnO_2$ electrodes via direct interfacial electron transfer without the use of electron mediators. Taking advantage from the optical transparency of the electrode we use optical absorbance spectroscopy to compliment the information obtained from electrochemical techniques.

Improved electronic coupling between the heme centre of MP-11and the electrode in comparison with HRP (from previous studies) on the same electrodes has been achieved [34]. However, since the heme is more exposed, its redox and other properties

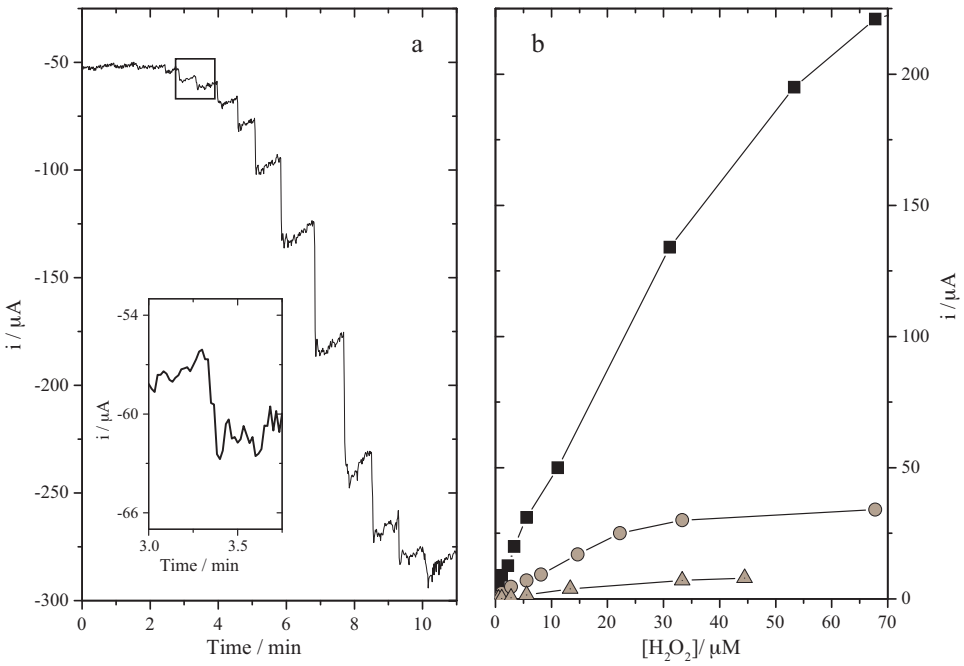


**Fig. 9.** (a) Chronoamperometric response of MP-11/$SnO_2$-PLL electrode under constant potential of −0.2 V in 0.01 M PBS, pH 8.0 to additions of $H_2O_2$ every 40 s. (b) Calibration curves of current response versus concentration of H2O2 for MP-11 (■) and HRP (○) modified $SnO_2$-PLL electrodes and blank electrode (△).

are more susceptible to the changing of the microenvironment at the interface. The first evidence of this is the red shift of the soret band of MP-11/$SnO_2$-PLL, mimicking those exhibited by low spin, six coordinated iron heme proteins [13,55,56]. Since titration of MP-11 solutions with PLL, PEI, and DDAB all induce the red shift in Soret band, this behaviour may be influenced by the polycation promoters rather than by the electrode.

Previous research has shown that this spin change can be induced by the binding of primary amines or hydroxyl ions at the sixth position of the iron centre coordination [13]. Although PLL and PEI have one primary amine in each monomer, it is quite unlikely that they are going to take part in iron ligation since at the working pH of 8, 99% of them are protonated. Moreover, DDAB does not have primary amines but is still able to induce the red shift. Therefore, the spectral shift is most likely due to the intermolecular binding of the MP-11, induced by the high local concentration of MP-11 on the electrode upon electrostatic binding of the hemepetide to the polycations. This seems to primarily proceed through the primary amine of the N-terminal residues ($pK_a \sim 7.5$). In addition, the involvement of lysine residues cannot be ruled out since positive microenvironment at the interface may also decrease the local $pK_a$ of the lys13 in MP-11 so that its proton affinity decreases and it therefore becomes deprotonated at the working pH of 8.

However, it is interesting to note that the midpoint potential of MP-11 on DDAB modified electrodes is almost 0.2 V more positive than those on PLL or PEI modified electrodes. Despite being observed for several bioelectrochemical systems (Mb, P450, HRP, MP-11, etc.), the explanation for this positive shift phenomenon remains unclear. Most probably, it is due to simply the combined influence of the positive and hydrophobic microenvironment provided by this cationic lipid bilayer. Positive environments may be expected to increase the electron affinity of a redox couple hence inducing some extra positive shift in $E_m$; a similarly hydrophobic environment may stabilise the heme porhyrin.

Furthermore, we address the influence of the microenvironment upon the catalytic activity of MP-11. We have demonstrated that the catalytic activity may result from an electrochemical analogue of Fenton reaction. CV data indicates direct involvement of Fe(III)/Fe(II) redox transition in $H_2O_2$ electrocatalysis in MP-11/$SnO_2$-PLL electrode systems. This observation was obtained regardless of the type of binding promoters used. Our data are very similar to literature studies of the electrocatalytic system employing Fe-EDTA, $H_2O_2$ and carbon electrode [57,58], suggesting an electrochemically controlled Fenton reaction:

$$Fe(II) + H_2O_2 \rightarrow Fe(III) + H_2O_2^{\bullet -} \rightarrow OH^- + OH^{\bullet}$$

Moreover, it is worth noting that regardless of the mechanism involved, we have demonstrated the feasibly of using peroxidase modified mesoporous metal oxide films electrodes as $H_2O_2$ biosensors for both optical and electrochemical sensing. A linear increase in current is observed as a function of $H_2O_2$ concentration, within a range 0.05–30 μM for MP-11 modified electrodes. However, our biosensor is better used as a disposable one. The immobilized MP-11 is partially destroyed/bleached by the increasing concentrations of $H_2O_2$.

## 5. Conclusion

MP-11 has been employed to functionalize mesoporous metal oxide electrodes. We have demonstrated that MP-11 is able to retain its redox activity upon immobilization. The catalytic activity of the immobilized MP-11 is found to proceed via the Fenton reaction, yielding OH radical intermediates. The viability of using this electrode system as a $H_2O_2$ biosensor has been demonstrated.

## Acknowledgement

Financial support from BBSRC is gratefully acknowledged.

## References

[1] M.P.J. Van Deurzen, F. van Rantwijk, R.A. Sheldon, Tetrahedron 53 (1997) 13183–13220.
[2] L. Gorton, A. Lindgren, T. Larsson, F.D. Munteanu, T. Ruzgas, I. Gazaryan, Anal. Chim. Acta 400 (1999) 91–108.
[3] P.A. Mabrouk, Anal. Chem. 68 (1996) 189–191.
[4] A. Walcarius, Electroanalysis 13 (2001) 701–718.

[5] B. Wang, B. Li, Z. Wang, G. Xu, S. Dong, Anal. Chem. 71 (1999) 1935–1939.
[6] S. Bharathi, M. Nogami, S. Ikeds, Langmuir 17 (2001) 1–4.
[7] Y. Xiao, H.X. Ju, H.Y. Chen, Anal. Biochem. 278 (2000) 22–28.
[8] H. Zimmermann, A. Lindgren, W. Schuhmann, L. Gorton, Chem. Eur. J. 6 (2000) 592–599.
[9] J. Aron, D.A. Baldwin, H.M. Marques, J.M. Pratt, P.A. Adams, J. Inorg. Biochem. 27 (1986) 227–243.
[10] J. Peterson, M.M.M. Saleem, J. Silver, M.T. Wilson, I.E.G. Morrison, J. Inorg. Biochem. 19 (1983) 165–178.
[11] J. Peterson, J. Silver, M.T. Wilson, I.E.G. Morrison, J. Inorg. Biochem. 13 (1980) 75–82.
[12] A. Ehrenberg, H. Theorell, Acta Chem. Scand. 9 (1955) 1193–1205.
[13] P.A. Adams, Peroxidases Chem. Biol. 2 (1991) 171–200.
[14] T. Loetzbeyer, W. Schuhmann, E. Katz, J. Falter, H.-L. Schmidt, J. Electroanal. Chem. 377 (1994) 291–294.
[15] W. Huang, Z. Zhang, X. Han, J. Tang, Z. Peng, S. Dong, E. Wang, Biophys. Chem. 94 (2001) 165–173.
[16] T. Tatsuma, T. Watanabe, Anal. Chem. 63 (1991) 1580–1585.
[17] V. Razumas, A. Gudavicius, J. Kazlauskaite, J. Kulys, J. Electroanal. Chem. Interfac. Electrochem. 271 (1989) 155–160.
[18] V. Razumas, T. Nylander, T. Arnebrant, J. Colloid Interface Sci. 164 (1994) 181–189.
[19] M. Delucchi, M. Panizza, J. Appl. Electrochem. 39 (2009) 2275–2284.
[20] D. O'Donoghue, E. Magner, Electrochim. Acta 53 (2007) 1134–1139.
[21] V. Razumas, J. Kazlauskaite, R. Vidziunaite, Bioelectrochem. Bioenerg. 39 (1996) 139–143.
[22] K.Q. Wang, Z.S. Ma, T.H. Lu, Chem. J. Chin. Univ.-Chin. 30 (2009) 553–556.
[23] Z. Qi, X. Li, D. Sun, C. Li, T. Lu, X. Ding, X. Huang, Bioelectrochemistry 68 (2006) 40–47.
[24] H.J. Jiang, Y. Zhao, H. Yang, Mater. Chem. Phys. 114 (2009) 879–883.
[25] J.J. Gooding, R. Wibowo, J. Liu, W. Yang, D. Losic, S. Orbons, F.J. Mearns, J.G. Shapter, D.B. Hibbert, J. Am. Chem. Soc. 125 (2003) 9006–9007.
[26] F. Mazzei, G. Favero, M. Frasconi, Chem. Eur. J. 15 (2009) 7359–7367.
[27] X. Zhu, I. Yuri, X. Gan, I. Suzuki, G. Li, Biosens. Bioelectron. 22 (2007) 1600–1604.
[28] S. Yabuki, F. Mizutani, Y. Hirata, J. Electroanal. Chem. 468 (1999) 117–120.
[29] L. Gorton, G. Bremle, E. Csoeregi, G. Joensson-Pettersson, B. Persson, Anal. Chim. Acta 249 (1991) 43–54.
[30] I. Willner, E. Katz, Angew. Chem. Int. Ed. 39 (2000) 1180–1218.
[31] E. Ferapontova, L. Gorton, Electroanalysis 15 (2003) 484–491.
[32] S. Yabuki, F. Mizutani, Y. Hirata, Electrochemistry (Tokyo) 68 (2000) 853–855.
[33] E. Topoglidis, Y. Astuti, F. Duriaux, M. Ratzel, J.R. Durrant, Langmuir 19 (2003) 6894–6900.
[34] Y. Astuti, E. Topoglidis, J.R. Durrant, Anal. Chim. Acta 648 (2009) 2–6.
[35] A. Lindgren, T. Ruzgas, L. Gorton, E. Csoregi, G. Bautista Ardila, I.Y. Sakharov, I.G. Gazaryan, Biosens. Bioelectron. 15 (2000) 491–497.
[36] E.E. Ferapontova, V.G. Grigorenko, A.M. Egorov, T. Borchers, T. Ruzgas, L. Gorton, Biosens. Bioelectron 16 (2001) 147–157.
[37] E.E. Ferapontova, V.G. Grigorenko, A.M. Egorov, T. Borchers, T. Ruzgas, L. Gorton, J. Electroanal. Chem. 509 (2001) 19–26.
[38] H.M. Khan, M. Anwar, G. Ahmad, J. Radioanal. Nucl. Chem. 200 (1995) 521–527.
[39] A.K. Collins, G.M. Makrigiorgos, G.K. Svensson, Med. Phys. 21 (1994) 1741–1747.
[40] S.C. Ashawa, U.R. Kini, U. Madhvanath, Int. J. Appl. Radiat. Isot. 30 (1979) 7–10.
[41] W.A. Armstrong, R.A. Facey, D.W. Grant, W.G. Humphreys, Can. J. Chem. 41 (1963) 1575–1577.
[42] M. Komatsu, T.N. Rao, A. Fujishima, Chem. Lett. 32 (2003) 396–397.
[43] E.N. Kadnikova, N.M. Kostic, J. Org. Chem. 68 (2003) 2600–2608.
[44] H.M. Goldston Jr., A.N. Scribner, S.A. Trammell, L.M. Tender, Chem. Commun. (2002) 416–417.
[45] S. Othman, A. Le Lirzin, A. Desbois, Biochemistry 32 (1993) 9781–9791.
[46] E. Ferapontova, Electroanalysis 16 (2004) 1101–1112.
[47] Y. Astuti, E. Topoglidis, G. Gilardi, J.R. Durrant, Bioelectrochemistry 63 (2004) 55–59.
[48] E. Laviron, J. Electroanal. Chem. Interfac. Electrochem. 101 (1979) 19–28.
[49] T Loetzbeyer, W. Schuhmann, H.L. Schmidt, Sens. Actuators B: Chem. B33 (1996) 50–54.
[50] J.F. Rusling, A.E.F. Nassar, J. Am. Chem. Soc. 115 (1993) 11891–11897.
[51] J.F. Rusling, A.E.F. Nassar, T.F. Kumosinski, ACS Symp. Ser. 576 (1994) 250–268.
[52] K.I. Ishibashi, A. Fujishima, T. Watanabe, K. Hashimoto, Electrochem. Commun. 2 (2000) 207–210.
[53] T. Ruzgas, E. Csoeregi, J. Emmneus, L. Gorton, G. Marko-Varga, Anal. Chim. Acta 330 (1996) 123–138.
[54] G. Presnova, V. Grigorenko, A. Egorov, T. Ruzgas, A. Lindgren, L. Gorton, Faraday Discuss. 116 (2000) 281–289.
[55] H.B. Dunford, Peroxidases Chem. Biol. 2 (1991) 1–24.
[56] H.R. Bosshard, H. Anni, T. Yonetani, Peroxidases Chem. Biol. 2 (1991) 51–84.
[57] R.M. Hutcheson, M.D. Engelmann, I.F. Cheng, BioMetals 18 (2005) 43–51.
[58] M.D. Engelmann, R.T. Bobier, T. Hiatt, I.F. Cheng, BioMetals 16 (2003) 519–527.